CAMERA BASED EVALUATION OF PHOTOMETRIC COMPENSATION METHODS ON MULTI-PROJECTOR DISPLAYS

Aditi Majumder

Department of Computer Science, University of California, Irvine.
majumder@ics.uci.edu

ABSTRACT

An important problem in achieving seamless multi-projector displays is the photometric (luminance) variation across the display. Currently, evaluation of the improvement in the quality of the imagery achieved by applying different photometric correction methods and a comparison between them is done by a subjective human user. In this paper, we present a camera-based method for relative evaluation of the luminance properties of the imagery on multi-projector displays, both before correction and after correction using different compensation techniques. To the best of our knowledge, this is the first camera-based method designed to evaluate the different photometric correction methods on a multi-projector display. We show that using our simple and automatic evaluation scheme the optimal photometric compensation parameter for a multi-projector display can be identified, which is not possible by subjective evaluation.

1. INTRODUCTION

Large high-resolution displays made of multiple projectors are becoming very popular [1, 2, 3, 4]. A critical obstacle towards making these displays seamless is to compensate for the non-uniform luminance (photometry) across the display [5]. Several camera-based methods exist [5, 6, 7] to correct this photometric variation. However, the evaluation of the quality of the improvement achieved by such methods and the comparison between the results achieved by different methods are done by a human and is hence subjective.

Existing image quality metrics [8, 9, 10, 11], used in graphics and vision, compare images against a golden reference. For example, for compression techniques, an uncompressed image is used as the golden reference to compare images compressed using different compression techniques. Similarly, for image synthesis, an image generated using global illumination methods is used as a golden reference. The problem faced while using such an algorithm to evaluate the results from different photometric correction techniques for large tiled displays, is the *lack of such a golden reference*. The input digital image when projected on the display and captured by a camera, goes through two different color spaces, one of the projector and the other of the camera. Hence, comparing the image captured by the camera with the input digital image does not make sense. Thus, this input digital image can not act as our golden reference.

In this paper, we make the first-attempt to develop a camera based relative evaluation technique for measuring the improvements achieved in photometric properties (like brightness and dynamic range) of the imagery on multi-projector display with the application of different photometric correction methods. Our method is simple, automatic and helps us to find optimal photometric compensation parameters and methods for a particular display.

2. GOAL

[12, 7] presents methods that correct the photometric variation in multi-projector displays by achieving photometric uniformity, that is, *identical* luminance response at every display pixel. However, since this method matches the response of the display with the 'worst possible pixel' ignoring all the 'good' pixels that are very much in the majority, it results in images of very low dynamic range and brightness. [6] shows that perceptual seamlessness can be achieved by just *smoothing* the luminance response across the display pixels, instead of making the response identical. A smoothing parameter λ is used to control the smoothness of the photometric response of the display. Increased smoothing leads to greater reduction in brightness and dynamic range, with the worst case being that of photometric uniformity with the smoothest (flat) luminance response (Figure 1).

Our goal is to use the camera to evaluate the properties of the display before and after photometric compensation. This will in turn enable us to evaluate the quality of the photometric correction achieved. A camera can measure a large range of luminance using varying exposure settings and hence, can be used for relative photometric evaluation of the display. However, the color of the projected image captured by the camera depends on camera and projector color gamuts, both of which can be significantly different from the gamut of the input image. Hence, this image can

0-7803-8554-3/04/$20.00 ©2004 IEEE.

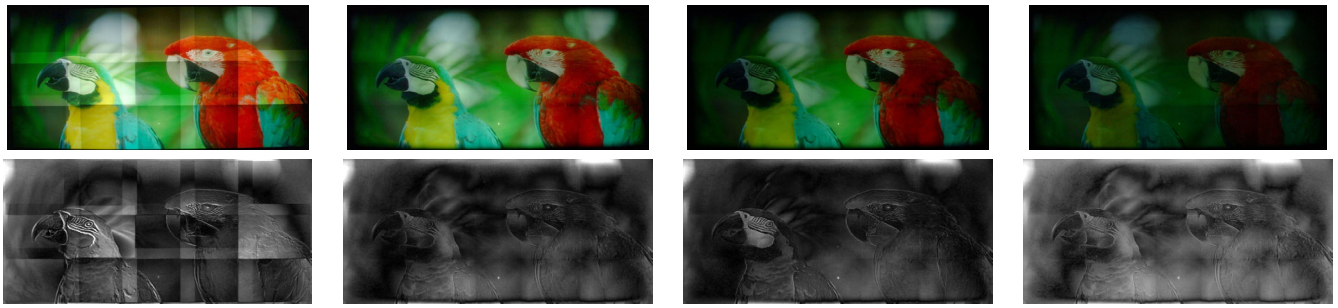

Fig. 1. Top: Digital photographs of a fifteen projector tiled display ($8' \times 10'$ in size) before any correction (left), after photometric response smoothing with parameter of $\lambda = 400$ (second), $\lambda = 800$ (third) and after photometric uniformity i.e. $\lambda = \infty$ (right). Note that the brightness and the dynamic range of the display reduces as the smoothing parameter increases. Bottom: Error images corresponding to the different color compensations of Figure 1 (1) Uncorrected display (E_1) (2) After photometric response smoothing with $\lambda = 400$ (E_2). (3) After photometric seamlessness with smoothing parameter $\lambda = 800$ (E_3). (4) After photometric response smoothing i.e $\lambda = \infty$ (E_4)

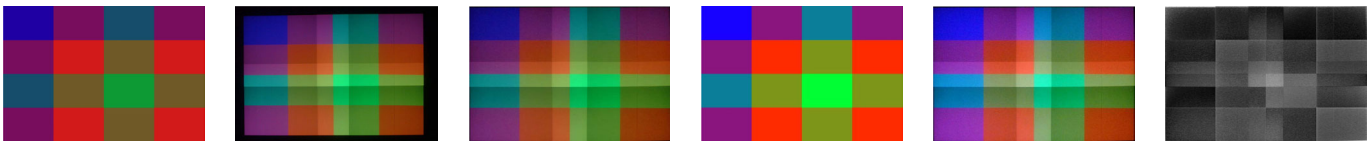

Fig. 2. From left: (1) Reference image, (2) Result image, (3) The recaptured image corresponding to the result image in (2), (4) Comparable reference image (Compare with (1) and note the increased brightness of the green channel due to the normalization of the channel range), (5) Comparable recaptured Image, (6) Error of the comparable recaptured image from the comparable reference image.

Img	$Brightness_i$	$Dynamic\ Range_i$	$Total\ Error_i$	$Mean\ Error_i$
R	$(125, 115, 81)$	$(236, 223, 231)$	NA	NA
O_1	$(106, 117, 66)$	$(248, 227, 241)$	251577	0.26
O_2	$(68, 92, 46)$	$(206, 227, 201)$	160942	0.16
O_3	$(63, 85, 42)$	$(195, 227, 172)$	146448	0.14
O_4	$(42, 65, 35)$	$(152, 220, 147)$	352060	0.35

Table 1. Results for the images shown in Figure 1

be significantly skewed in color when compared to the input image. The goal is to extract reasonable information about the photometric appearance of the display being insensitive to the camera and projector color spaces. Thus, our evaluation metric should (1) bring the input image and the images of the display captured by a camera within a common reference frame so that they can be compared, and (2) indicate how the dynamic range, brightness and general photometric appearance of the input image is affected by the correction.

3. ALGORITHM OVERVIEW

Let the input image be called the *reference image* R. We would like to compare this image with the image captured by a camera of the input image projected on an uncorrected or photometrically corrected display.

3.1. Geometric Comparability

First, we run a geometric calibration algorithm with the camera at location A. The geometric calibration information relates the projector coordinates with the global display coordinates through the camera coordinates. Any existing geometric calibration method [13, 14, 15] can be used for this purpose. Next, keeping the camera in the same location A, we take the images of the display when R is projected on it. This image is called the *result image* and is denoted by O_C. The geometric calibration information is then used to convert O_C into the display coordinate space. Also, to remove the effect of the photometric non-linearity of the camera, the inverse of the camera response function is applied to this image. The camera response function is recovered apriori using high dynamic range imaging method [16]. The image thus generated from O_C is called *recaptured image* and is denoted by O. Note that O and R now have the same resolution and are geometrically comparable pixel by pixel. (Figure 2).

We may have more than one recaptured image if we are trying to compare different algorithms. Thus, for generality we denote each of these by O_i (Figure 3). All the result images corresponding to the O_is should be captured with the same camera settings and from the same location A to

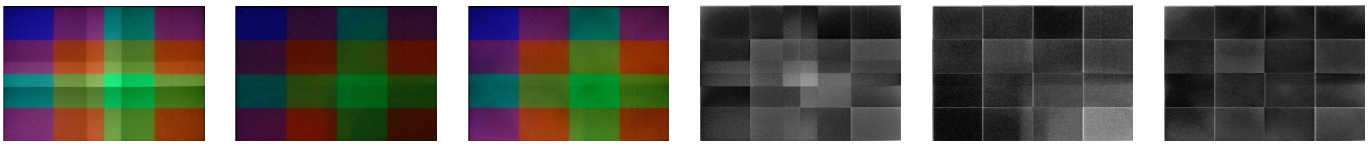

Fig. 3. From left: (1) Recaptured image before correction (O_1) (2) Recaptured image after photometric uniformity ($\lambda = \infty$) (O_2). (3) Recaptured image after achieving photometric response smoothing with $\lambda = 400$ (O_3). (4) Error image for uncorrected display (E_1). (5) Error image for photometric uniformity (E_2). (6) Error image for photometric response smoothing with $\lambda = 400$. (E_3). The reference image R is the same as in Figure 2

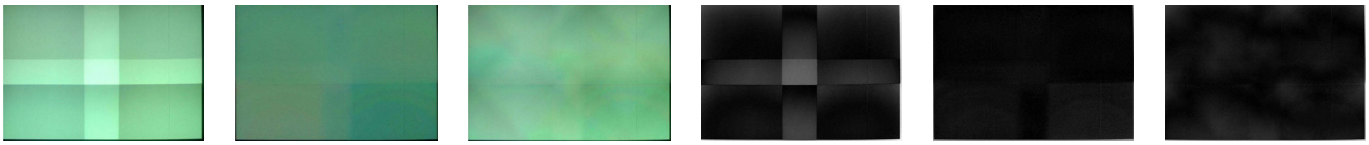

Fig. 4. From Left: (1) Recaptured image with uncorrected display (O_1) (2) Recaptured image after photometric uniformity ($\lambda = \infty$) (O_2). (3) Recaptured image after photometric response smoothing with $\lambda = 400$ (O_3). (4) E_1. (5) E_2. (6) E_3.

Img	$Brightness_i$	$Dynamic\ Range_i$	$Total\ Error_i$	$Mean\ Error_i$
R	$(115, 51, 66)$	$(197, 154, 136)$	NA	NA
O_1	$(88, 83, 67)$	$(209, 240, 159)$	60962	0.25
O_2	$(41, 39, 30)$	$(121, 137, 111)$	56223	0.23
O_3	$(75, 67, 51)$	$(174, 168, 155)$	45766	0.18

Table 2. Results for the images shown in Figure 3

Img	$Brightness_i$	$Dynamic\ Range_i$	$Total\ Error_i$	$Mean\ Error_i$
R	$(255, 255, 255)$	$(0, 0, 0)$	NA	NA
O_1	$(135, 204, 160)$	$(60, 90, 70)$	30049	0.12
O_2	$(76, 135, 105)$	$(30, 20, 20)$	14214	0.06
O_3	$(117, 182, 137)$	$(40, 60, 50)$	13887	0.05

Table 3. Results for the images shown in Figure 4

be comparable. However, note that the R and the O_is are still not photometrically comparable.

3.2. Photometric Comparability

For photometric comparability, we first find the mean of all the pixels for R and O_i denoted by B_R and B_{O_i} respectively. This indicates the *brightness* of these images. Next, for each R and O_i we define a deviation image given by the vector deviation of the color at each pixel from the corresponding means, B_R and B_{O_i} respectively. This deviation images are called R^D and O_i^D. Next, we do the following for each channel l.

(1) We find the maximum and minimum of *all* pixels across *all* the images (O_i^Ds and R^D), denoted by l_m and l_M respectively.

(2) Then, we normalize the range of values in *each* of the O_i^Ds and R^D within l_m and l_M. The corresponding images thus generated, denoted by R^M and O_i^Ms, are called *comparable reference image* and *comparable recaptured images* respectively (Figure 2). The difference between the maximum and minimum for each channel across each of R^M and O_i^M defines their respective *dynamic range* vector DR.

This step translates the range of all the images to a common reference frame. Now, O^{M_i}s and R^M are photometrically comparable even if they are generated from incomparable R^D and O_i^Ds.

Error Images Generation: Next we generate the error image E_i corresponding to each O_i by finding the normalized pixel-wise Euclidian distance between R^M and O_i^M, as shown in Figure 3. The sum and mean of E_i, denoted by TE_i and ME_i respectively, gives the *total* and the *mean* error of O_i from R .

Error Metric: The brightness (B), dynamic range (DR) and error images (E) comprise our error metric. Note that there may not be any physical O_i that can exactly resemble R. This method only brings R and O_is in a similar reference frame in terms of per channel luminance values relative to the camera. Hence, the success of a correction method lies in reducing the errors rather than eliminating them.

3.3. Evaluation Results

Figure 3 shows the reference and recaptured images that we want to compare. In this case, they are images taken before correction (O_1), after photometric uniformity (O_2), and then after smoothing photometric response with $\lambda = 400$ (O_3). The corresponding error images are E_1, E_2 and E_3. Table 2 summarizes the error metric. As expected, the brightness, dynamic range, TE and ME for O_2 is higher than that of O_3. Figure 4 and Table 3 show the same for a flat white reference image. Notice how the camera color

gamut can change the color appearance of the O_is significantly, but it does not affect our evaluation technique. Figure 1 and Table 1 shows the results for a fifteen projector display where O_{1-4} are respectively the images before correction, after smoothing with parameter 400 and 800, and after photometric uniformity.

Note that the error TE and ME is high with an uncorrected display and becomes smaller with the increase in λ. In this phase, change in appearance due to the presence of sharp luminance variation plays a dominant role in generating the error. However, at some point the error reaches a minimum, after which it increases with increase in λ being very high for $\lambda = \infty$ (Table 1). In this phase, change in appearance due to the compression in the dynamic range is the dominant factor. Thus, the error signifies the change in photometric appearance that can occur due to different reasons. This change in error with changing λ is plotted in Figure 5. Thus, this quantitative evaluation technique helps us to find the ideal smoothing parameter where the error is minimum which cannot be done by subjective evaluation.

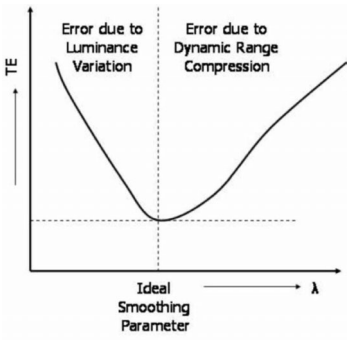

Fig. 5. Error vs Smoothing Parameter.

4. CONCLUSION

In conclusion, we present a novel camera based evaluation method to judge the results from different photometric compensation methods on multi-projector display. We show that such a evaluation technique help us to identify the optimal compensation parameters and methods.

5. REFERENCES

[1] M. Hereld, I.R. Judson, and R.L. Stevens, "Introduction to building projector-based tiled display systems," *IEEE Computer Graphics and Applications*, pp. 22–28, 2000.

[2] Kai Li, Han Chen, Yuqun Chen, Douglas W. Clark, Perry Cook, Stefanos Damianakis, Georg Essl, Adam Finkelstein, Thomas Funkhouser, Allison Klein, Zhiyan Liu, Emil Praun, Rudrajit Samanta, Ben Shedd, Jaswinder Pal Singh, George Tzanetakis, and Jiannan Zheng, "Early experiences and challenges in building and using a scalable display wall system," *IEEE Computer Graphics and Applications*, vol. 20(4), pp. 671–680, 2000.

[3] G. Humphreys and P. Hanrahan, "A distributed graphics system for large tiled displays," in *Proceedings of IEEE Visualization*, 1999.

[4] Ruigang Yang, David Gotz, Justin Hensley, Herman Towles, and Michael S. Brown, "Pixelflex: A reconfigurable multi-projector display system," *Proceedings of IEEE Visualization*, 2001.

[5] Aditi Majumder and Rick Stevens, "Color nonuniformity in projection-based displays: Analysis and solutions," *Transactions of Visualization and Computer Graphics (to appear)*, 2003.

[6] Aditi Majumder, "A practical framework to achieve perceptually seamless multi-projector displays, phd thesis," Tech. Rep., University of North Carolina at Chapel Hill, 2003.

[7] Andrew Raij, Gennette Gill, Aditi Majumder, Herman Towles, and Henry Fuchs, "Pixelflex2: A comprehensive, automatic, casually-aligned multi-projector display," *IEEE International Workshop on Projector-Camera Systems*, 2003.

[8] Jeffrey Lubin, "A visual discrimination model for imaging system design and evaluation," *Vision Models for Target Detection and Recognition, Editor: E. Peli, World Scientific*, pp. 245–283, 1995.

[9] Scott Daly, "The visual differences predictor : An algorithm for the assessment of image fidelity," *Digital Images and Human Vision, Editor: A.B.Watson, MIT Press*, pp. 179–206, 1993.

[10] Mahesh Ramasubramanian, S. N. Pattanaik, and Donald P. Greenberg, "A perceptually based physical error metric for realistic image synthesis," *Proceedings of SIGGRAPH'99*, pp. 73–82, 1999.

[11] James Ferwerda, S.N. Pattanaik, Peter Shirley, and Donald P. Greenberg, "A model of visual masking for computer graphics," *Proceedings of SIGGRAPH'97*, pp. 143–152, 1997.

[12] Aditi Majumder and Rick Stevens, "LAM: Luminance attenuation map for photometric uniformity in projection based displays," *Proceedings of ACM Virtual Reality and Software Technology*, 2002.

[13] Mark Hereld, Ivan R. Judson, and Rick Stevens, "Dottytoto: A measurement engine for aligning multi-projector display systems," *Projection Displays IX, Proceedings of SPIE Vol. 5002, ed. Ming Hsien Wu, Santa Clara, CA*, 2003.

[14] Ramesh Raskar, "Immersive planar displays using roughly aligned projectors," in *Proceedings of IEEE Virtual Reality 2000*, 1999.

[15] Han Chen, Rahul Sukthankar, Grant Wallace, and Kai Li, "Scalable alignment of large-format multi-projector displays using camera homography trees," *Proceedings of IEEE Visualization*, 2002.

[16] Paul E. Debevec and Jitendra Malik, "Recovering high dynamic range radiance maps from photographs," *Proceedings of ACM Siggraph*, pp. 369–378, 1997.